SIAM J. SCI. COMPUT.
Vol. 19, No. 1, pp. 155–171, January 1998

012

NUMERICAL CONFORMAL MAPPING METHODS FOR SIMPLY AND DOUBLY CONNECTED REGIONS*

THOMAS K. DELILLO† AND JOHN A. PFALTZGRAFF‡

Abstract. Methods are presented and analyzed for approximating the conformal map from the interior (exterior) of the disk to the interior (exterior) of a smooth, simple closed curve and from an annulus to a bounded, doubly connected region with smooth boundaries. The methods are Newton-like methods for computing the boundary correspondences and conformal moduli similar to Fornberg's method for the interior of the disk. We show that the linear systems are discretizations of the identity plus a compact operator and, hence, that the conjugate gradient method converges superlinearly.

Key words. numerical conformal mapping, doubly connected regions, Fornberg's method, compact operators, conjugate gradient method

AMS subject classifications. 30C30, 65E05

PII. S1064827596303545

1. Introduction.

Introductions to numerical conformal mapping can be found in the texts [Ga] and [He]. For simply connected regions with smooth boundaries, a number of methods which map from the unit disk to the region and employ the fast Fourier transform (FFT) are available [De], [DE1], [Fo1], [Weg1], [Weg2], [Weg4]. For doubly connected regions with smooth boundaries, methods which use the annulus as a computational domain and employ FFTs are given in [Fo2], [LM], [Weg3]. Several of these methods are Newton-like methods for computing the boundary correspondence. It can be shown for the interior disk case [Fo1], [Weg4] that the matrices for the inner systems are discretizations of the identity plus a compact operator and that the conjugate gradient method therefore converges superlinearly [Weg2], [Wid]. In this paper we extend this analysis to Fornberg's method for the exterior of the disk and to the annulus where a Newton-like version of [Fo2] is given.

Currently the most robust and stable methods for the disk are based on solving Riemann–Hilbert problems for the Newton updates. In [Weg4], a discrete interpolation problem is solved, and in [Weg5] (which can be specialized to the disk), damping of higher-order Fourier coefficients is used to avoid the instabilities in [Weg1]; see, e.g., [De], [DE1]. In both cases convergence of the numerical method is proved. It is not known to us whether these methods generalize to the doubly connected cases or whether [LM] or [Weg3] suffer from instabilities like [Weg1].

The Fornberg-like methods below generalize to a variety of computational domains, such as ellipses [DE2], [Weg5], cross-shaped regions [DEP], and multiply connected circle domains (work in progress). These methods are based on finding analyticity conditions for the computational domains and provide, we believe, an interesting class of problems for conjugate gradient-like methods. In section 2 of this paper, we define certain useful linear operators. In section 3, we state the analyticity conditions

*Received by the editors May 15, 1996; accepted for publication (in revised form) March 6, 1997. http://www.siam.org/journals/sisc/19-1/30354.html

†Department of Mathematics and Statistics, Wichita State University, Wichita, KS 67260-0033 (delillo@twsuvm.uc.twsu.edu). The research of this author was partially supported by U. S. Department of Energy grant DE-FG02-92ER25124 and National Science Foundation EPSCoR grant OSR-9255223.

‡Department of Mathematics, The University of North Carolina at Chapel Hill, CB 3250, Phillips Hall, Chapel Hill, NC 27599-3250 (jap@math.unc.edu).

for the interior of the disk, the exterior of the disk, and the annulus. In section 4, we derive a slightly modified version of Fornberg's method for the interior of the disk [Fo1]. We review the analysis of the method given in [Weg2] and [Wid] and give a more thorough discussion of the eigenvalue structure of the discrete equations. In sections 5 and 6, we discuss the exterior disk and annulus maps, respectively.

2. Linear operators. We have need of several operators occurring in Fourier analysis; see, e.g., [Weg2]. We take the domain of these operators to be the set of 2π-periodic functions h in L^2. Let

$$h(\theta) = \sum_{k=-\infty}^{\infty} a_k e^{ik\theta}.$$

Then the conjugation operator, K, is given by

$$Kh(\theta) = \frac{1}{2\pi} P.V. \int_0^{2\pi} \cot\left(\frac{\theta-\phi}{2}\right) h(\phi) d\phi = \sum_{k=-\infty}^{-1} ia_k e^{ik\theta} - \sum_{k=1}^{\infty} ia_k e^{ik\theta},$$

$$Jh(\theta) = \frac{1}{2\pi} \int_0^{2\pi} h(\theta) d\theta = a_0,$$

$$P_+ h = \frac{1}{2}(I + iK - J)h = \sum_{k=1}^{\infty} a_k e^{ik\theta}, \quad P_- h = \frac{1}{2}(I - iK + J)h = \sum_{k=-\infty}^{0} a_k e^{ik\theta}.$$

We will also make use of the discretizations of the operators above using N-point trigonometric interpolation. If

$$\underline{h} = (h_0, \ldots, h_{N-1})^T, \; h_k = h(\theta_k), \; \theta_k = 2\pi k/N, \; k = 0, \ldots, N-1,$$

and

$$\hat{a}_k = \frac{1}{N} \sum_{j=0}^{N-1} h_j w^{-jk}, \; w = e^{2\pi i/N},$$

then with $n = N/2$ the trigonometric polynomial interpolating h is given by

$$T_N h(\theta) = \sum_{k=-n+1}^{n-1} \hat{a}_k e^{ik\theta} + \hat{a}_n \cos(n\theta),$$

and the discrete operators corresponding to those introduced above are

$$K_N h(\theta) = \sum_{k=-n+1}^{-1} i\hat{a}_k e^{ik\theta} - \sum_{k=1}^{n-1} i\hat{a}_k e^{ik\theta},$$

$$J_N h(\theta) = \hat{a}_0 - \hat{a}_n \cos(n\theta),$$

and

$$P_{+,N} h = \frac{1}{2}(T_N + iK_N - J_N)h = \sum_{k=1}^{n-1} \hat{a}_k e^{ik\theta} + \hat{a}_n \cos n\theta,$$

$$P_{-,N} = \frac{1}{2}(T_N - iK_N + J_N) = \sum_{k=-n+1}^{0} \hat{a}_k e^{ik\theta}.$$

If the $N \times N$ matrix $F := (w^{-k\nu}),\ k, \nu = 0, \ldots, N-1$, then

$$\frac{1}{N} F \underline{h} = \underline{a} = (\hat{a}_0, \ldots, \hat{a}_{N-1})^T = (\hat{a}_0, \ldots, \hat{a}_n, \hat{a}_{-n+1}, \ldots, \hat{a}_{-1})^T$$

since $\hat{a}_k = \hat{a}_{k-N}$. Note that

$$\frac{1}{N} F^H F = \frac{1}{N} F F^H = I_N \quad (H = \text{Hermitian transpose}).$$

In matrix form

$$P_{-,N} = \frac{1}{N} F^H I_{-,N} F, \quad P_{+,N} = \frac{1}{N} F_N^H I_{+,N} F,$$

where $I_{-,N} = \mathrm{diag}(1, 0, \ldots, 0, 1, \ldots, 1)$ and $I_{+,N} = \mathrm{diag}(0, 1, \ldots, 1, 0, \ldots, 0)$ are $N \times N$ diagonal matrices of rank n.

3. Analyticity conditions. We will use the following conditions; see, e.g., [He, sec. 14.3.I].

THEOREM. *A function $f \in \mathrm{Lip}(C)$ on the boundary C of the unit disk extends to an analytic function in the interior of the disk with $f(0) = 0$ if and only if*

$$P_- f(e^{i\theta}) = 0. \tag{1}$$

THEOREM. *A function $f \in \mathrm{Lip}(C)$ on the boundary C of the unit disk extends to an analytic function in the exterior of the disk with $f(\infty)$ finite if and only if*

$$P_+ f(e^{i\theta}) = 0. \tag{2}$$

THEOREM. *Consider an annulus $\rho < |z| < 1$ with boundaries $C = C_1 - C_2$ where $C_1 : e^{i\theta}, C_2 : \rho e^{i\theta}, 0 < \rho < 1$. Then $f \in \mathrm{Lip}(C)$ extends analytically to the annulus if and only if*

$$\int_{C_1} f(z) z^k dz = \int_{C_2} f(z) z^k dz,\ k = 0, \pm 1, \pm 2, \ldots.$$

Then for

$$f(e^{i\theta}) = \sum_{k=-\infty}^{\infty} a_k e^{ik\theta},$$

$$f(\rho e^{i\theta}) = \sum_{k=-\infty}^{\infty} b_k e^{ik\theta},$$

we have

$$\rho^k a_k = b_k,\ k = 0, \pm 1, \pm 2, \ldots. \tag{3}$$

4. Fornberg's method for simply connected regions interior to a Jordan curve. Here we rederive the Newton-like method [Fo1] for the interior of the disk. We recall the analysis of [Weg2], [Wid] and give a more complete discussion of the eigenvalue structure of the inner linear systems.

We wish to find the conformal map f from the interior of the unit disk to the interior of a smooth Jordan curve $\Gamma : \gamma(S)$ parametrized by, for instance, arclength

S with $f(0) = 0$ and $f'(0) > 0$ or $f(1)$ fixed. In this case, f extends smoothly to the boundary and $f(e^{i\theta}) = \gamma(S(\theta))$. The numerical problem is to approximate the *boundary correspondence* $S(\theta)$. This will yield an approximation to the Taylor series $f(z) = \sum_{k=1}^{\infty} a_k z^k$. Newton-like methods can be used for determining $S(\theta)$. At the kth Newton step a correction $U^{(k)}(\theta)$ real to $S^{(k)}(\theta)$ is computed from the condition that the linearization

$$f(e^{i\theta}) \approx \xi(\theta) + e^{i\beta(\theta)} U^{(k)}(\theta), \tag{4}$$

where $\xi(\theta) = \gamma(S^{(k)}(\theta))$ and $\beta(\theta) = \arg \gamma'(S^{(k)}(\theta))$, extends analytically to the interior of the unit disk with $f(0) = 0$. From the analyticity conditions in section 3, we have

$$2P_{-} f = (I - iK + J) f = 0. \tag{5}$$

This implies (with $U = U^{(k)}$) that

$$(I - iK + J) e^{i\beta(\theta)} U(\theta) = -2P_{-}\xi(\theta). \tag{6}$$

Using U real gives

$$(I + R^{in}) U = r \tag{7}$$

where $R^{in} = \mathrm{Re}(e^{-i\beta}(J - iK)e^{i\beta})$ and $r = -\mathrm{Re}(e^{-i\beta}(I - iK + J)\xi)$.

R^{in} can be represented as a Fredholm integral operator on $L^2(0, 2\pi)$ with kernel

$$R(\theta, \phi) = \frac{1}{2\pi} \sin\left(\beta(\phi) - \beta(\theta) + \frac{(\theta - \phi)}{2}\right) \Big/ \sin\left(\frac{(\theta - \phi)}{2}\right). \tag{8}$$

For γ sufficiently smooth R^{in} is a symmetric, compact operator on L^2; see [Weg2, sec. 4], [Wid]. With $E = \mathrm{diag}_j(e^{i\beta(\theta_j)}), j = 0, 1, \ldots, N-1$, discretization with N-point trigonometric interpolation gives

$$(I_N + R_N)\underline{U} = \underline{r}. \tag{9}$$

The matrix

$$I_N + R_N = \frac{2}{N} \mathrm{Re}(E^H F^H I_{-,N} F E) \tag{10}$$

is symmetric, positive (semi)definite with eigenvalues well grouped around 1, as we will show below, and thus the conjugate gradient method converges superlinearly. The FFT is used to perform the matrix–vector multiplications in $O(N \log N)$. The Newton update is given by $\underline{S}^{(k+1)} = \underline{S}^{(k)} + \underline{U}^{(k)}$ and we set $U_0 = 0$ to fix a boundary point as in [Fo1]. Equation (9) is a slight reformulation of [Fo1]. In [DEP], we report computations which use the conjugate gradient method to solve (9).

The eigenvalue structure of the matrix R_N can be understood in terms of that of R^{in}. Some results on this have been given in [Weg2] and [Wid]. Here we give a more complete discussion. In [Weg2, sect. 5] (see also [Weg4, sect. 6.1]) it is shown that the matrix $R_N = (r_{lk})$ has a checkerboard structure,

$$r_{lk} = \begin{cases} 0, & l - k \text{ even}, \\ \frac{1}{n} \frac{\sin(\beta_k - \beta_l + (\theta_l - \theta_k)/2)}{\sin((\theta_l - \theta_k)/2)}, & l - k \text{ odd}, \end{cases}$$

where $\beta_k := \beta(\theta_k)$, so that the block structure

$$P^T R_N P = \begin{pmatrix} 0 & R_1 \\ R_1^T & 0 \end{pmatrix}$$

can be given, where P is the permutation matrix such that

$$P^T \underline{U} = \begin{pmatrix} \underline{U}_o \\ \underline{U}_e \end{pmatrix}$$

and $\underline{U}_o, \underline{U}_e$ are the odd and even indexed components of $\underline{U}$, respectively. It is well known that if λ is an eigenvalue of R_N, i.e., $\lambda \in \sigma(R_N)$, then $-\lambda \in \sigma(R_N)$, and $\lambda^2 \in \sigma(R_1^T R_1)$, In fact, if

$$\begin{pmatrix} 0 & R_1 \\ R_1^T & 0 \end{pmatrix} \begin{pmatrix} \underline{U}_o \\ \underline{U}_e \end{pmatrix} = \begin{pmatrix} R_1 \underline{U}_e \\ R_1^T \underline{U}_o \end{pmatrix} = \lambda \begin{pmatrix} \underline{U}_o \\ \underline{U}_e \end{pmatrix},$$

then

$$\begin{pmatrix} 0 & R_1 \\ R_1^T & 0 \end{pmatrix} \begin{pmatrix} \underline{U}_o \\ -\underline{U}_e \end{pmatrix} = -\lambda \begin{pmatrix} \underline{U}_o \\ -\underline{U}_e \end{pmatrix} \tag{11}$$

and

$$\begin{pmatrix} 0 & R_1 \\ R_1^T & 0 \end{pmatrix}^2 \begin{pmatrix} \underline{U}_o \\ \underline{U}_e \end{pmatrix} = \begin{pmatrix} R_1 R_1^T & 0 \\ 0 & R_1^T R_1 \end{pmatrix} \begin{pmatrix} \underline{U}_o \\ \underline{U}_e \end{pmatrix} = \lambda^2 \begin{pmatrix} \underline{U}_o \\ \underline{U}_e \end{pmatrix}. \tag{12}$$

We want to relate $\sigma(R_N)$ to the spectrum $\sigma(R^{in})$ of R^{in} which has been dealt with in [Weg2]. It was shown there that -1 is a simple eigenvalue of R^{in}, $|\lambda| < 1$ for the other eigenvalues, and for $0 < |\lambda| < 1, -\lambda$ is also an eigenvalue. In order to state our theorem we need to establish some notation. We want to apply the theory of collectively compact operators from Anselone [An] and Atkinson [At] to accomplish our goal. This requires some analysis since the approximation of R^{in} obtained by trigonometric interpolation is not an approximation by the Nyström method, so that the results of [An] and [At] do not apply directly. In our problem the relevant Nyström operator is given by

$$R^{(n)} u(\theta) = \sum_{j=1}^{n} \frac{2\pi}{n} R(\theta, \theta_{2j}) u(\theta_{2j}),$$

that is, by approximation by the trapezoidal rule with $n = N/2$. It follows from [An, Prop 2.2, p. 19] that $\{R^{(n)}\}$ is a collectively compact approximation to the compact operator R^{in}, and from [An, Theorem 4.8, p. 65] that $\sigma(R^{(n)}) \to \sigma(R^{in})$ in the sense that every neighborhood of $\sigma(R^{in})$ contains $\sigma(R^{(n)})$ for n sufficiently large. If $\lambda \in \sigma(R^{(n)})$, that is, $R^{(n)} u(\theta) = \lambda u(\theta)$, we have, in particular, by setting $\theta = \theta_{2i}$, that $\lambda \in \sigma(R_2)$ where the $n \times n$ matrix $R_2 := (\frac{2\pi}{n} R(\theta_{2i}, \theta_{2j}))$. Using this notation we have the matrix $R_1 = (\frac{2\pi}{n} R(\theta_{2i-1}, \theta_{2j}))$, and in order to apply the above theory we need to relate $\sigma(R_1)$ and $\sigma(R_2)$ for n large. After doing this we will be able to prove the following theorem.

THEOREM 1. $\sigma(R_1) \to \sigma(R^{in})$.

Proof. If β is sufficiently smooth, R will be differentiable. Then by the mean value theorem, we can write

$$\frac{2\pi}{n}(R(\theta_{2i-1}, \theta_{2j}) - R(\theta_{2i}, \theta_{2j})) = c_{ij}/n^2$$

where c_{ij} is bounded, and $R_1 = R_2 + \delta R$, $\delta R_{ij} = c_{ij}/n^2$. Since R_2 is real and symmetric there is an orthogonal matrix Q diagonalizing R_2 and the Bauer–Fike theorem [GVL, p. 342] implies that, for $\mu \in \sigma(R_1)$,

$$\min_{\lambda \in \sigma(R_2)} |\lambda - \mu| = \|\delta R\|_2.$$

Since, by [GVL, p. 57],

$$\|\delta R\|_2 \le n \max_{i,j} |\delta R_{ij}|,$$

we have

$$\min_{\lambda \in \sigma(R_2)} |\lambda - \mu| = O\left(\frac{1}{n}\right). \qquad \square$$

Using similar ideas we can show that $\sigma(R_1^T) \to \sigma(R^{in})$, $\sigma(R_1 R_1^T) \to \sigma((R^{in})^2)$, $\sigma(R_1^T R_1) \to \sigma((R^{in})^2)$, and, most usefully, $\sigma(R_N) \to \sigma(R^{in}) \cup \sigma(-R^{in}) = \sigma(R^{in}) \cup \{1\}$. These facts are needed in our discussion of convergence of the conjugate gradient method below.

Now we will discuss the implementation of the condition $U_0 = 0$, which yields the normalization condition $f(1) = \gamma(0)$, and the effects of the normalization conditions on the eigenvalue distribution of $I_N + R_N$. The eigenvalues are computed with the NAGLIB routine F02AAF. The matrix-vector multiplications in the conjugate gradient routine are performed with the radix-2 complex FFT routine from [DB, p. 416].

From above, we see that $\hat{a}_k = 0$, $k = -n+1, \ldots, 0$, $\underline{a} = \frac{1}{N} F \underline{h}$, $\underline{h} = \underline{\xi} + E\underline{U}$ may be written as

$$C\underline{U} = -(I_1 \ I_2) F \underline{\xi} =: \underline{c} \tag{13}$$

where $C = (I_1 \ I_2) FE$ and I_1 and I_2 are as the $n \times n$ matrices diag(1,0,. . . ,0) and diag(0,1,. . . ,1), respectively. Let $\underline{q}^T = (1, 0, \ldots, 0)$. Then the condition $U_0 = 0$ is given by $\underline{q}^T \underline{U} = \delta$ where $\delta = 0$. Now let

$$D = \begin{pmatrix} C \\ \sqrt{N} \underline{q}^T / 2 \end{pmatrix}, \qquad \underline{g} := \begin{pmatrix} \underline{c} \\ \delta \end{pmatrix}. \tag{14}$$

Equation (13) and the normalization then give

$$D\underline{U} = \underline{g}, \tag{15}$$

a system of $N/2$ complex equations, and one real equation for the N real unknowns, $\underline{U}$. A calculation shows that

$$\frac{2}{N} \mathrm{Re}(D^H D) = \frac{2}{N} \mathrm{Re}(C^H C) + \frac{1}{2} \underline{q}\underline{q}^T = I_N + R_N + \frac{1}{2} \underline{q}\underline{q}^T. \tag{16}$$

Since $\underline{U}$ is real, the normal equations give the $N \times N$ real system

$$(I_N + R_N)\underline{U} + \frac{1}{2} \underline{q}\underline{q}^T \underline{U} = \underline{r} := \frac{2}{N} \mathrm{Re}(D^H \underline{g}). \tag{17}$$

This system contains the normalization condition $U(0) = 0$ and should have full rank. (We note that the standard alternative normalization condition for f, $f'(0) > 0$, which implies Im $a_1 = 0$ could also be expressed in the form $\underline{q}^T \underline{U} = \delta$ for suitable $\underline{q}^T$ and δ, but we have not used this in our computations.)

We can now make some observations on the eigenvalues of $\frac{2}{N}\mathrm{Re}(D^H D)$. Note that the $\frac{1}{2}\underline{qq}^T$ could be replaced by $\epsilon \underline{qq}^T$ for any $\epsilon > 0$. Then $\epsilon \underline{qq}^T \underline{q} = \epsilon \underline{q}$, and so ϵ is an eigenvalue and $\underline{q}$ an eigenvector of $\epsilon \underline{qq}^T$. Also, 0 is an eigenvalue of $\epsilon \underline{qq}^T$ of multiplicity $N-1$. Since $I_N + R_N$ and $\epsilon \underline{qq}^T$ are symmetric, we have from, e.g., [GVL, Cor. 8.1.3, p. 411], that

$$\lambda_k(I_N + R_N) \le \lambda_k \left(\frac{2}{N} \mathrm{Re}(D^H D) \right) \le \lambda_k(I_N + R_N) + \epsilon, \tag{18}$$

where $\lambda_k(A)$ is the kth smallest eigenvalue of A. These relations have indeed been observed computationally. We also observe that the eigenvalues interlace according to [GVL, Cor. 8.1.5, pp. 411–412] or [Lu, p. 276], so that

$$\lambda_k(I_N + R_N) \le \lambda_k \left(\frac{2}{N} \mathrm{Re}(D^H D) \right) \le \lambda_{k+1}(I_N + R_N). \tag{19}$$

As an example, first let us consider the case where Ω is the unit disk. Let R_1 be as above. Then

$$R_1 = (r_{2i-1,2j}) = \left(-\frac{2}{N} \right).$$

(This is incorrectly given in [Fo1, p. 392] and [Wid, p. 13] as $-1/N$.) With $\underline{r} = (1, 1, \ldots, 1)^T$, we have $R_1 \underline{r} = -\underline{r}$ and rank(R_1)= 1. Therefore the eigenvalues of R_1 are -1 and 0 with multiplicity $n-1$. From equation (11), we see that the eigenvalues of $I_N + R_N$ are 0, 1, and 2 with multiplicities 1, $N-2$, and 1, respectively. Table 1 lists some sample eigenvalue calculations with and without the normalization term.

Another example given in Table 1 is the case where Ω is an ellipse of minor to major axis ratio $\alpha = .8$. With $N = 32$, 2 and 0 are eigenvalues of $I_N + R_N$, and the other eigenvalues occur in pairs of multiplicity 2 of the form $\lambda = 1 \pm r$, clustering around 1, as expected from $\sigma(R_N) \to \sigma(R^{in}) \cup \{1\}$. If $\frac{1}{2}\underline{qq}^T$ is added to $I_N + R_N$, we find that the eigenvalues $\lambda_1 = 0$ and λ_N are perturbed by $O(1/N)$ and the pairs are split with the lower values remaining fixed and the upper values increasing slightly as seen in the table. The conjugate gradient method required about seven or fewer iterations to reduce the residuals to less than 10^{-15}. For $\alpha = .8$ there are seven eigenvalues with $|\lambda_k - 1| \ge .1$, so this gives a good indication of the rate of convergence.

As α for the ellipse decreases, the upper and lower eigenvalues smear out toward 0 and 2, as seen in Table 1 for $\alpha = .4$, but the spectrum remains well grouped around 1. There is a corresponding slight increase in the number of conjugate gradient iterations. For instance, for $\alpha = .4$ there are 10 eigenvalues with $|\lambda_k - 1| \ge .1$, and roughly 10 conjugate gradient iterations are taken at each Newton step. The conjugate gradient method generally finds $\underline{U}$ accurately in several iterations with only slight dependence on the geometry of the region. More detailed estimates of the superlinear convergence could be obtained from estimates of the decay rates of the eigenvalues of the compact operators, such as [Weg2, Theorem 4], and standard estimates of the convergence of the conjugate gradient method in terms of eigenvalues; see, e.g., [SW]. For instance, for an ellipse we would expect to find r-superlinear convergence with the residuals at the kth step of the form $O(r^{k^2})$ for some $0 < r < 1$ and $r \uparrow 1$ as $\alpha \downarrow 0$. Similar results should hold for other elongated or thin regions where some "thinness" parameter α

TABLE 1
Eigenvalues for disk map.

Ω	k	$\lambda_k(I_N + R_N)$	$\lambda_k(\frac{2}{N}\mathrm{Re}(D^H D))$
Unit disk $N = 32$	1	0.	.01
	2	1.	1.
	$\vdots$	$\vdots$	$\vdots$
	30	1.	1.
	31	1.	1.46
	32	2.	2.03
Ellipse $\alpha = .8$ $N = 32$	1	0.	.021
	2	.674	.674
	3	.674	.697
	4	.987	.987
	5	.987	.989
	$\vdots$	$\vdots$	$\vdots$
	28	1.012	1.012
	29	1.012	1.231
	30	1.326	1.326
	31	1.326	1.494
	32	2.000	2.056
Ellipse $\alpha = .4$ $N = 128$	1	0.	.030
	2	.082	.082
	3	.082	.210
	4	.884	.884
	5	.884	.896
	6	.926	.926
	7	.926	.944
	$\vdots$	$\vdots$	$\vdots$
	122	1.074	1.074
	123	1.074	1.088
	124	1.116	1.116
	125	1.116	1.161
	126	1.918	1.918
	127	1.918	1.953
	128	2.000	2.204

approaches 0 (see [De] for several explicit examples). We will not pursue this further here, except to say that the conformal mapping problem itself becomes highly ill conditioned due to the *crowding phenomenon* for small α, requiring very large values of N to achieve even a small amount of accuracy. For instance, an ellipse with $\alpha = .2$ is a very difficult region for a Fourier series map, independently of the method used, so that the question of the convergence rates of the conjugate gradient method is a somewhat moot point in this case. As we will see below, the situation for the annulus is slightly more complicated.

Addition of the normalization term $\epsilon \underline{q}\underline{q}^T$, $\epsilon > 0$, is generally necessary. For instance, the method converged for ellipses of $\alpha = .8$ and .6 with $\epsilon = 0$, but did not converge for $\alpha = .4, \epsilon = 0$. With $\epsilon = .5$ the method converged in all these cases. Other $\epsilon > 0$ also are suitable and do not affect the convergence rates as standard estimates for the conjugate gradient method indicate; see, e.g., [Lu, Chap. 8] or [Ax, sect. 4.1].

We note that our eigenvalue study is similar to that of Fornberg [Fo1]. Fornberg's $n \times n$ matrix $G = I - R_1 R_1^T$, and he imposes the normalization by fixing $U_0 = 0$ and using the conjugate gradient method on an $(n-1) \times (n-1)$ principal submatrix $\hat{G}$ of

G. The eigenvalues of $\hat{G}$ then interlace those of G according to [GVL, Cor. 8.1.4, p. 411]. For more discussion of the eigenvalues and normalization conditions, see [Weg2] and [Weg4].

5. Fornberg-like method for simply connected regions exterior to a Jordan curve. Here we extend the method [Fo1] for the interior of the disk to the exterior case. The analysis for the interior carries over to the exterior case.

Now we wish to find the conformal map f from the exterior of the unit disk to the exterior of a smooth Jordan curve $\Gamma : \gamma(S)$ parametrized by, for instance, arclength S with $f(\infty) = \infty$ and $f'(\infty) > 0$ or $f(1)$ fixed. In this case, f extends smoothly to the boundary and $f(e^{i\theta}) = \gamma(S(\theta))$. The numerical problem is again to approximate the *boundary correspondence* $S(\theta)$. This will yield an approximation to the Laurent series $f(z) = a_1 z + a_0 + \sum_{k=1}^{\infty} a_{-k} z^{-k}$. The setup is similar to the interior case. At the kth Newton step a correction $U^{(k)}(\theta)$ real to $S^{(k)}(\theta)$ is computed from the condition that the linearization

$$h(e^{i\theta}) = \xi(\theta) + e^{i(\beta(\theta)-\theta)} U^{(k)}(\theta) \approx f(e^{i\theta}) e^{-i\theta}, \tag{20}$$

where $\xi(\theta) = \gamma(S^{(k)}(\theta)) e^{-i\theta}$ and $\beta(\theta) = \arg \gamma'(S^{(k)}(\theta))$, extends analytically to the exterior of the unit disk with h analytic at ∞. From (2), we have

$$2P_+ h = (I + iK - J)h = 0. \tag{21}$$

This implies (with $U = U^{(k)}$) that

$$(I + iK - J) e^{i(\beta(\theta)-\theta)} U(\theta) = -2P_+ \xi(\theta). \tag{22}$$

Using U real gives

$$(I + R^{ex})U = r \tag{23}$$

where $R^{ex} = \mathrm{Re}(e^{-i(\beta-\theta)}(iK - J)e^{i(\beta-\theta)})$ and $r = -\mathrm{Re}(e^{-i(\beta-\theta)}(I + iK - J)\xi)$. For γ sufficiently smooth R^{ex} is a compact operator on L^2; see [Weg2, sect. 4], where $R^{ex} = -R_V = \mathrm{Re}(\overline{V}(iK - J)V),\ V = e^{i(\beta-\theta)}$.

Note that R^{ex} can be represented as a Fredholm integral operator on $L^2(0, 2\pi)$ with kernel

$$R(\theta, \phi) = \frac{1}{2\pi} \sin(\beta(\phi) - \beta(\theta) + 3(\theta - \phi)/2) / \sin((\theta - \phi)/2). \tag{24}$$

With $E = \mathrm{diag}_j(e^{i(\beta_j - \theta_j)}), j = 0, 1, \ldots, N-1$, discretization with N-point trigonometric interpolation gives

$$(I_N + R_N^{ex})\underline{U} = \underline{r}. \tag{25}$$

The matrix

$$I_N + R_N^{ex} = \frac{2}{N} \mathrm{Re}(E^H F^H I_{+,N} F E) \tag{26}$$

is thus symmetric with eigenvalues well grouped around 1, and the conjugate gradient method converges superlinearly. The FFT is used to perform the matrix–vector multiplications in $O(N \log N)$. The Newton update is the same as the interior case, and we again set $U_0 = 0$ to fix a boundary point.

6. Fornberg-like method for bounded, doubly connected regions. In this section, we generalize [Fo1] to doubly connected regions. Fornberg himself extended his method to the doubly connected case [Fo2]. He solves a system of equations [Fo2, eq. (6)], which are essentially our analyticity conditions, using a linearly convergent method of successive approximation. Here we show how to linearize these equations to get a quadratically convergent, Newton-like method. We derive a symmetric linear system which is a discretization of the identity plus a compact operator, and so the conjugate gradient method converges superlinearly (with a dependence on ρ as observed below) with $O(N \log N)$ matrix–vector multiplications using the FFT. Our linearization is that used by Luchini and Manzo [LM]; however, they solve Riemann–Hilbert problems for the Newton updates. Wegmann [Weg3] also solves Riemann–Hilbert problems, but uses a slightly different and more expensive linearization.

If the target region Ω is bounded by two smooth Jordan curves $\Gamma_1 : \gamma_1(S_1)$ and $\Gamma_2 : \gamma_2(S_2)$, we want to find the *boundary correspondences* $S_1(\theta)$ and $S_2(\theta)$ and the *conformal modulus* ρ such that $f(z)$ is analytic in the annulus $\rho < |z| < 1$ and $f(e^{i\theta}) = \gamma_1(S_1(\theta))$ and $f(\rho e^{i\theta}) = \gamma_2(S_2(\theta))$. We have programmed a Newton-like method to do this. At each Newton step we want to compute corrections $U_1(\theta),\ U_2(\theta)$, and $\delta\rho$ to $S_1(\theta),\ S_2(\theta)$, and ρ. With arclength, $S_j,\ \beta_j(\theta) := \arg \gamma_j'(S_j(\theta)),\ \xi_j(\theta) := \gamma_j(S_j(\theta)),\ j = 1, 2,\ \zeta(\theta) := f'(\rho e^{i\theta})e^{i\theta} = -ie^{i\beta_2(\theta)} dS_2(\theta)/d\theta/\rho$, as in [LM] we linearize about S_1, S_2 as follows:

$$f(e^{i\theta}) = \xi_1(\theta) + e^{i\beta_1(\theta)}U_1(\theta), \tag{27}$$

$$f(\rho e^{i\theta}) = \xi_2(\theta) + e^{i\beta_2(\theta)}U_2(\theta) - \zeta(\theta)\delta\rho. \tag{28}$$

For the annulus, it is easier to begin with the discrete equations. We discretize the analyticity conditions (3) and apply them to linearizations (27), (28) with N-point trigonometric interpolation to get a discrete approximation to the U_j's at the Fourier points, $\theta_k = 2\pi k/N, k = 0, 1, \ldots, N-1$. Letting a_k and b_k now denote the N discrete Fourier coefficients and using the N-periodicity $a_{k+N} = a_k$, we have with $N = 2n$

$$\underline{a} = (a_0, a_1, \ldots, a_n, a_{n+1}, \ldots, a_{N-1})^T = (a_0, a_1, \ldots, a_n, a_{-n+1}, \ldots, a_{-1})^T.$$

$\underline{b}$ is defined similarly. Next define the $N \times N$ matrices $P_1 = \text{diag}(1, \rho, \ldots, \rho^{n-1}, 1, \ldots, 1)$ and $P_2 = -\text{diag}(1, \ldots, 1, 1, \rho^{n-1}, \ldots, \rho)$. If we set $a_n = b_n$ as in [Fo2, eq. 6], we write the discrete form of our analyticity conditions as

$$P_1\underline{a} + P_2\underline{b} = 0. \tag{29}$$

With $E_j := \text{diag}_{l=0,\ldots,N-1}(e^{i\beta_j(\theta_l)}),\ j = 1, 2$, our discrete linearizations become

$$N\underline{a} = F\underline{\xi}_1 + FE_1\underline{U}_1, \tag{30}$$

$$N\underline{b} = F\underline{\xi}_2 + FE_2\underline{U}_2 - F\underline{\zeta}\delta\rho. \tag{31}$$

Substituting these linearizations into the discrete analyticity conditions gives our linear system for $\underline{U}_1,\ \underline{U}_2$, and $\delta\rho$,

$$(C\ \underline{w})\underline{U} = P_1FE_1\underline{U}_1 + P_2FE_2\underline{U}_2 - P_2F\underline{\zeta}\delta\rho = -P_1F\underline{\xi}_1 - P_2F\underline{\xi}_2 =: \underline{c}, \tag{32}$$

where $C = (P_1 F E_1 \ P_2 F E_2)$ is a complex $N \times 2N$ matrix, $\underline{w} = -P_2 F \underline{\zeta}$ is a complex N-vector, and

$$\underline{U} = \begin{pmatrix} \underline{U}_1 \\ \underline{U}_2 \\ \delta\rho \end{pmatrix}.$$

Equation (32) is a system of N complex equations in $2N+1$ real unknowns, $\underline{U}$. To satisfy the normalization $f(1) = \gamma_1(0)$, we add the equation $\underline{q}^T \underline{U} = U_0 = \delta := 0$, where $\underline{q}^T = (1, 0, \ldots, 0)^T$ is a $2N+1$-vector. Similarly to (14), we write

$$D = \begin{pmatrix} \frac{C}{\sqrt{N}} & \underline{w} \\ & \underline{q}^T/2 \end{pmatrix}, \qquad \underline{g} := \begin{pmatrix} \underline{c} \\ \delta \end{pmatrix}, \tag{33}$$

and our system now becomes

$$D\underline{U} = \underline{g}, \tag{34}$$

a system of N complex equations and one real equation for the $2N+1$ real unknowns, $\underline{U}$. Using the normal equations and $\underline{U}$ real, we have

$$\frac{2}{N}\mathrm{Re}(D^H D)\underline{U} = \underline{r} := \frac{2}{N}\mathrm{Re}(D^H \underline{g}). \tag{35}$$

As in the simply connected case, we solve (35) by the conjugate gradient method using FFTs. This system contains the normalization condition $U_0 = 0$ and should have full rank. However, as we see below, numerically the rank is only $2N$. It is easy to see that the matrices (36) and (37) are symmetric, positive semidefinite. The discrete analyticity conditions lead to a matrix (36) below with a zero eigenvalue of multiplicity 2, and fixing a boundary point only gets rid of one zero eigenvalue. We presently see no easy way to fill this gap. Nonetheless, the effect on the numerics appears to be small. The conjugate gradient method reduces the residuals in the inner iterations, and the Newton steps converge to the correct solution for sufficiently large N and for a reasonable initial guess.

Now we will analyze (35) more carefully and show that the matrix is a discretization of the identity plus a compact operator as in the disk case. We have the following $2N+1 \times 2N+1$ matrix:

$$\frac{2}{N}\mathrm{Re}(D^H D) = \begin{pmatrix} A_{11} & A_{12} & \underline{w}_1 \\ A_{12}^T & A_{22} & \underline{w}_2 \\ \underline{w}_1^H & \underline{w}_2^H & 2\underline{w}^H\underline{w}/N \end{pmatrix} + \frac{1}{2}\underline{q}\underline{q}^T, \tag{36}$$

where $A_{ij} = \frac{2}{N}\mathrm{Re}(E_i^H F^H P_i P_j F E_j)$ and $\underline{w}_i = \frac{2}{N}\mathrm{Re}(E_i^H F^H P_i \underline{w}),\ i, j = 1, 2$. We also note that the $2N \times 2N$ matrix containing the analyticity conditions is given by

$$\frac{2}{N}\mathrm{Re}(C^H C) = \begin{pmatrix} A_{11} & A_{12} \\ A_{12}^T & A_{22} \end{pmatrix}. \tag{37}$$

Now it is easy to see that A_{11} is a (low rank perturbation of) the discretization of

$$2\mathrm{Re}(e^{-i\beta_1}(P_- + l_1 *)e^{i\beta_1}) = I + R_1 + C_1 \tag{38}$$

with N-point trigonometric interpolation where $R_1 = \mathrm{Re}(e^{-i\beta_1}(J - iK)e^{i\beta_1})$ is compact, $*$ is convolution, $l_1(\theta) = \rho^2 e^{i\theta}/(1-\rho^2 e^{i\theta}) = \sum_{k=1}^{\infty} \rho^{2k} e^{ik\theta}$, and $C_1 = 2\mathrm{Re}(e^{-i\beta_1} l_1 *$

$(e^{i\beta_1}))$ is the product of bounded operators and a convolution and is, hence, compact. Similarly, A_{22} is also the discretization of

$$2\mathrm{Re}(e^{-i\beta_2}(P_+ + J + l_2*)e^{i\beta_2}) = I + R_2 + C_2, \tag{39}$$

where $R_2 = \mathrm{Re}(e^{-i\beta_2}(iK+J)e^{i\beta_2})$, $l_2(\theta) = \rho^2 e^{-i\theta}/(1-\rho^2 e^{-i\theta}) = \sum_{k=1}^{\infty} \rho^{2k} e^{-ik\theta}$, and $C_2 = 2\mathrm{Re}(e^{-i\beta_2} l_2 * (e^{i\beta_2}))$, and A_{12} is the discretization of an operator of the form $C_3 + C_4$, where $C_3 = -2\mathrm{Re}(e^{-i\beta_1} l_3 * (e^{i\beta_2}))$ and $C_4 = -2\mathrm{Re}(e^{-i\beta_1} l_4 * (e^{i\beta_2}))$ with $l_3(\theta) = 1/(1-\rho e^{i\theta}) = \sum_{k=0}^{\infty} \rho^k e^{ik\theta}$ and $l_3(\theta) = \rho e^{-i\theta}/(1-\rho e^{-i\theta}) = \sum_{k=1}^{\infty} \rho^{-k} e^{-ik\theta}$. Therefore (36) is a symmetric low rank perturbation of the discretization of the identity plus a compact operator. The eigenvalues cluster around 1. However, this case is more complicated than the case for the disk. As the examples in Tables 2a and b illustrate, the clustering is tighter as $\rho \downarrow 0$ and the conjugate gradient iterations converge rapidly. As $\rho \uparrow 1$, the eigenvalues spread out more, and more conjugate gradient iterations are required. These effects might be expected from the form of the $A_{i,j}$ matrices. Perhaps for values of ρ near 1, a preconditioner would be useful, but we will not pursue this here. We note that this effect is unrelated to the conditioning of the conformal mapping problem. For instance, the Joukowski ellipse with $\alpha_1 = .5$ and $\alpha_2 = .3$ in Figure 1b is well conditioned, but $\rho = .786\ldots$ and the conjugate gradient iterations converge slowly. It is not always necessary, however, to take many conjugate gradient steps in every inner system to get the outer Newton iterations to converge.

The Newton update at the kth Newton step is

$$\begin{aligned}
\underline{S}_1^{(k+1)} &= \underline{S}_1^{(k)} + \underline{U}_1^{(k)}, \\
\underline{S}_2^{(k+1)} &= \underline{S}_2^{(k)} + \underline{U}_2^{(k)}, \\
\rho^{(k+1)} &= \rho^{(k)} + \delta\rho^{(k)}.
\end{aligned}$$

The Newton iterations converge quadratically. The method is sensitive to the initial guess like Fornberg's method for the disk. We plan to report more extensive calculations with this method in a future paper. However, we give some examples here.

(i) *Annulus*. In this case $f(z) = z$. As a simple test case, we take the target region to be the annulus $\Omega = \{z : 0 < \rho < |z| < 1\}$ and the initial guess for the computational annulus to be $\{z : 0 < \rho^{(0)} < |z| < 1\}$. Suppose initially $\rho^{(0)} \neq \rho$, but $S_1^{(0)}(\theta) = \theta$ and $S_2^{(0)}(\theta) = \rho\theta$, the exact boundary correspondences for the outer and inner boundaries. We find that $\rho^{(k)} \to \rho$ quadratically, if $\rho^{(0)}$ and ρ do not differ too much. For instance, with $\rho^{(0)} = .1$ and $\rho = .9$, the method failed to converge. Note, in this case, $a_1 = 1, b_1 = \rho, a_k = b_k = 0, k \neq 1$, and $\zeta(\theta) = \rho e^{i\theta}/\rho^{(0)}$. Assuming $\underline{U}_1 = \underline{U}_2 = \underline{0}$, the linear system reduces to

$$\frac{\rho}{\rho^{(0)}} \delta\rho^{(0)} = -\rho^{(0)} a_1 + b_1 = -\rho^{(0)} + \rho.$$

Continuing, we get

$$\delta\rho^{(k)} = \frac{\rho^{(k)}}{\rho}(\rho - \rho^{(k)}), \quad k \geq 0,$$

and therefore

$$\rho - \rho^{(k+1)} = \rho - \rho^{(k)} - \delta\rho^{(k)} = \frac{1}{\rho}(\rho - \rho^{(k)})^2,$$

clearly displaying the quadratic convergence.

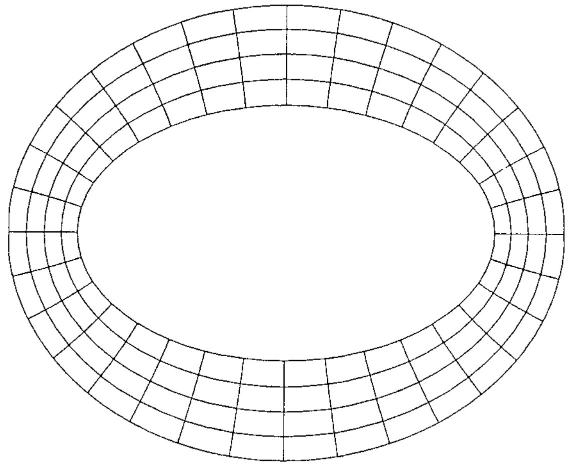

FIG. 1A. *Example* (ii), *Joukowski map,* $\alpha_1 = .8$, $\alpha_2 = .6$, $\rho = .666, \ldots, N = 128$.

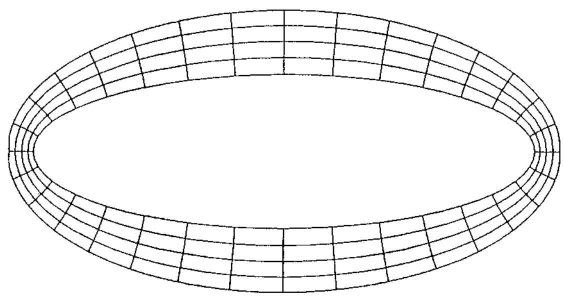

FIG. 1B. *Example* (ii), *Joukowski map,* $\alpha_1 = .5$, $\alpha_2 = .3$, $\rho = .7867, \ldots, N = 128$.

We can find the null vectors of $\frac{2}{N}\mathrm{Re}(C^H C)$ for the annulus. In this case $E_1 = E_2 = i\mathrm{diag}_{j=0,\ldots,N-1}(e^{ij2\pi/N})$. Now let $\underline{e}_+^T := (1, 1, \ldots, 1)^T$ and $\underline{e}_-^T := (1, -1, 1, -1, \ldots, 1, -1)^T$ be N-vectors. A straightforward calculation shows that the $2N$ vectors, $(\underline{e}_+^T, \rho \underline{e}_+^T)^T$ and $(\rho^{n-1}\underline{e}_-^T, \underline{e}_-^T)^T$, are real null vectors of $C^H C$ and hence real eigenvectors of $\frac{2}{N}\mathrm{Re}(C^H C)$ with zero eigenvalues. From our numerical results, zero appears to be an eigenvalue of multiplicity exactly 2 in all the examples we have checked so far.

(ii) *Joukowski ellipses*; see Figures 1a and 1b. In this example we use the Joukowski transformation, $g(z) = z + 1/z$, to produce a region Ω interior to confocal ellipses, Γ_1 and Γ_2 of minor-to-major axis ratios α_1 and α_2, respectively. We scale the ellipses such that the major axis of the outer ellipse is $[-1,1]$ and the map f is normalized by $f(1) = 1$. The boundaries are fitted with a periodic, cubic spline parametrized by (chordal) arclength. This provides a good approximation to arclength, and the loss of regularity does not have a serious effect up to the level of the error in the spline fit. (The method can be revised to use arbitrary parametrization S of the boundary.) We use the standard initial guess, such that $S_1^{(0)}(\theta_i)$ and $S_2^{(0)}(\theta_i)$ are distributed uniformly along Γ_1 and Γ_2 in arclength. We find that the method again converges quadratically if $S_1^{(0)}, S_2^{(0)}$, and $\rho^{(0)}$ are sufficiently close to the exact values. For instance, if $\alpha_1 = .6$ and $\alpha_2 = .4$ ($\rho = .7637626\ldots$), then with $\rho^{(0)} = .5$

TABLE 2A
Eigenvalues for Joukowski ellipses.

Ω	k	$\lambda_k(\frac{2}{N}\mathrm{Re}(C^H C))$	$\lambda_k(\frac{2}{N}\mathrm{Re}(D^H D))$
Joukowski	1	0.	0.
ellipses	2	0.	.008
$\alpha_1 = .999$	3	.351	.351
$\alpha_2 = .9$	4	.367	.370
$N = 64$	5	.396	.396
$\rho = .0974923$	6	.397	.407
	7	.906	.905
	$\vdots$	$\vdots$	$\vdots$
	119	1.009	1.009
	120	1.009	1.101
	121	1.103	1.102
	122	1.103	1.824
	123	2.000	2.019
	124	2.019	2.080
	125	2.580	2.595
	126	2.603	2.650
	127	2.650	2.657
	128	2.657	2.664
	129		127.9

the method converges. However, if $\alpha_1 = .9$ and $\alpha_2 = .2$ ($\rho = .2809757\ldots$), then with $\rho^{(0)} = .5$ and $N = 64$ the method fails to converge. Such (not extreme) sensitivity to the initial is probably to be expected, since Fornberg's method for the disk [Fo1] exhibits the same sensitivity. It should be possible to deal with this problem in most cases, by continuation from more nearly annular regions or by applying preliminary, explicit, osculation maps [He, 17.2] to make the region more nearly annular, as we remark in example (iv), below.

Next we give some numerical data. Tables 2a and 2b illustrate the dependence of the eigenvalues of the linear operators on ρ, as mentioned above. The number of conjugate gradient iterations needed to reduce the 2-norm of the residuals to a fixed level grew as $\rho \uparrow 1$ and the eigenvalues became less well grouped around 1. As a result, very rapid superlinear convergence rates are only clearly observed for cases such as Table 3, where $\rho = .097\ldots$. An example of the discretization error of the map, measured by the max norm of the error at the mesh point, is given in Table 4. Note that none of our examples are highly ill-conditioned conformal maps. An example of a doubly connected region which exhibits severe ill-conditioning due to crowding would be an elongated ellipse with a small hole in the center. We plan to study more examples in future work.

(iii) *Outer ellipse and translated and rotated inner ellipse;* see Figure 2. Here the outer ellipse has a minor-to-major axis ratio of $\alpha_1 = .9$ and the conformal map fixes $f(1) = 1$ at the end of the major axis. The inner ellipse has a minor-to-major axis ratio of $\alpha_2 = .5$ and is shrunk by a factor .5, rotated by an angle $\pi/8$, and translated by .1. With $N = 128$, we find $\rho = .401\ldots$, $S_1(0) = 0$, and $S_2(0) = -.130\ldots$. If the rotation is $\pi/5$, the method does not converge. If the condition $U_0 = 0$ is not used the method also fails to converge. Both ellipses are parametrized so that $\gamma_1(0)$ and $\gamma_2(0)$ are at the right ends of the major axes.

(iv) *Spline curve;* see Figure 3. The inner and outer boundaries here were each produced by placing 800 points in the plane and interpolating them with a periodic cu-

TABLE 2B
Eigenvalues for Joukowski ellipses.

Ω	k	$\lambda_k(\frac{2}{N}\mathrm{Re}(C^H C))$	$\lambda_k(\frac{2}{N}\mathrm{Re}(D^H D))$
Joukowski	1	0.	0.
ellipses	2	0.	.004
$\alpha_1 = .8$	3	.064	.064
$\alpha_2 = .6$	4	.145	.154
$N = 64$	5	.286	.261
$\rho = .666\ldots$	6	.300	.309
	7	.347	.350
	8	.388	.388
	9	.473	.473
	10	.475	.483
	11	.624	.624
	12	.624	.630
	13	.738	.738
	14	.738	.742
	15	.820	.820
	16	.820	.824
	17	.878	.878
	18	.878	.880
	19	.918	.918
	$\vdots$	$\vdots$	$\vdots$
	110	1.087	1.128
	111	1.132	1.132
	112	1.132	1.196
	113	1.201	1.201
	114	1.201	1.301
	115	1.310	1.310
	116	1.310	1.465
	117	1.483	1.483
	118	1.483	1.694
	119	1.768	1.768
	120	1.768	1.845
	121	2.000	2.066
	122	2.243	2.246
	123	2.248	2.272
	124	2.403	2.490
	125	2.862	2.862
	126	2.872	2.878
	127	2.955	2.982
	128	3.217	3.217
	129		106.6

TABLE 3
Conjugate gradient iterations for Joukowski ellipses, $\alpha_1 = .999,\ \alpha_2 = .9$.

Iter.	Residual error
1	$.77 \cdot 10^{-2}$
2	$.78 \cdot 10^{-3}$
3	$.32 \cdot 10^{-5}$
4	$.68 \cdot 10^{-5}$
5	$.29 \cdot 10^{-8}$
6	$.92 \cdot 10^{-10}$
7	$.17 \cdot 10^{-12}$
8	$.77 \cdot 10^{-13}$
9	$.35 \cdot 10^{-14}$
10	$.35 \cdot 10^{-14}$
11	$.11 \cdot 10^{-14}$
12	$.35 \cdot 10^{-15}$

TABLE 4
Accuracy for Joukowski ellipse, $\alpha_1 = .8, \alpha_2 = .6$.

N	Discr. error
32	$.40 \cdot 10^{-5}$
64	$.48 \cdot 10^{-8}$
128	$.22 \cdot 10^{-10}$

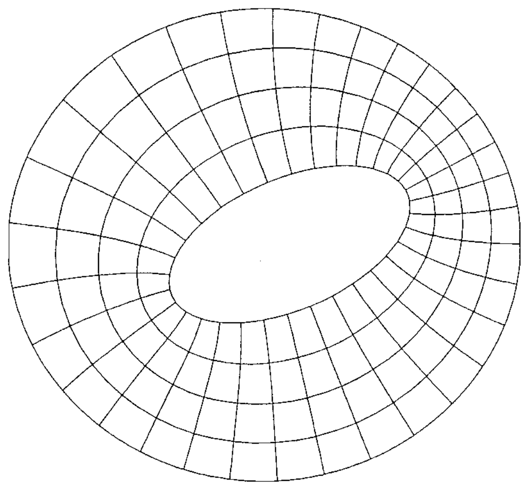

FIG. 2. *Example* (iii)*, rotated and translated ellipses,* $N = 128$.

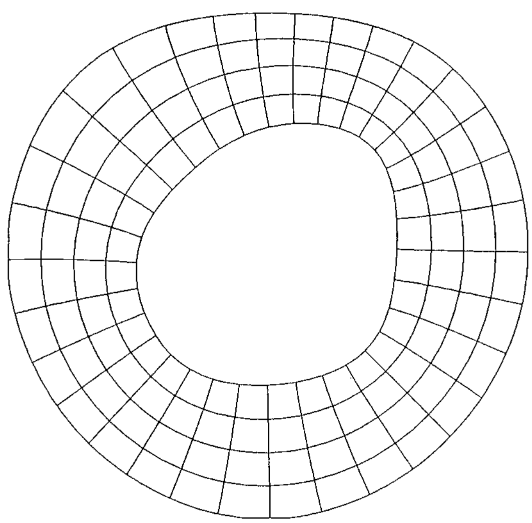

FIG. 3. *Example* (iv)*, spline boundaries,* $N = 128$.

bic spline parametrized by (chordal) arclength. We believe this to be a useful example, since boundary curves may not generally be given by analytic formulas in practice. For the simply connected case, Wegmann's original method [Weg1] often failed to converge for such boundaries. However, Fornberg's method [Fo1] and Wegmann's discrete methods [Weg4] and [Weg5] do converge. For doubly connected regions that are not nearly annular, osculation maps [Hoi], [He] can be applied to map a number of boundary points to nearly annular curves, and those boundary points can be fitted with splines. A good initial guess will then be available for our annulus method. We have used a similar procedure with osculation maps for simply connected regions [Gr], [He] combined with [Fo1], [Weg4], or [Weg5] (specialized to the disk) effectively. However, [Weg4] and [Weg5] do not generally require good initial guesses. [Fo1] and [Fo2] use continuation for regions which are not nearly circular or annular. (The present authors do not know how [LM] and [Weg3] perform in these cases.)

Acknowledgment. The authors thank Olof Widlund for useful discussions and the referees for suggesting a number of improvements.

REFERENCES

[An] P. M. Anselone, *Collectively Compact Operator Approximation Theory*, Prentice–Hall, Englewood Cliffs, NJ, 1971.

[At] K. E. Atkinson, *A Survey of Numerical Methods for the Solution of Fredholm Integral Equations of the Second Kind*, SIAM, Philadelphia, PA, 1976.

[Ax] O. Axelsson, *Solution of linear systems of equations: Iterative methods*, in Sparse Matrix Techniques, V. A. Barker, ed., Lecture Notes in Math. 572, Springer-Verlag, New York, 1977, pp. 1–51.

[DB] G. Dahlquist and Å. Björck, *Numerical Methods*, Prentice–Hall, Englewood Cliffs, NJ, 1974.

[De] T. K. DeLillo, *The accuracy of numerical conformal mapping methods: A survey of examples and results*, SIAM J. Numer. Anal., 31 (1994), pp. 788–812.

[DE1] T. K. DeLillo and A. R. Elcrat, *A comparison of some numerical conformal mapping methods for exterior regions*, SIAM J. Sci. Comput., 12 (1991), pp. 399–422.

[DE2] T. K. DeLillo and A. R. Elcrat, *A Fornberg-like conformal mapping method for slender regions*, J. Comput. Appl. Math., 46 (1993), pp. 49–64.

[DEP] T. K. DeLillo, A. R. Elcrat, and J. A. Pfaltzgraff, *Numerical conformal mapping methods based on Faber series*, J. Comput. Appl. Math., to appear.

[Fo1] B. Fornberg, *A numerical method for conformal mappings*, SIAM J. Sci. Statist. Comput., 1 (1980), pp. 386–400.

[Fo2] B. Fornberg, *A numerical method for conformal mapping of doubly connected regions*, SIAM J. Sci. Statist. Comput., 4 (1984), pp. 771–783.

[Ga] D. Gaier, *Konstruktive Methoden der konformen Abbildung*, Springer-Verlag, Berlin, Göttingen, Heidelberg, 1964.

[GVL] G. Golub and C. Van Loan, *Matrix Computations*, 2nd ed., The Johns Hopkins University Press, Baltimore, MD, 1989.

[Gr] E. Grassmann, *Numerical experiments with a method of successive approximation for conformal mapping*, Z. Angew. Math. Phys., 30 (1979), pp. 873–884.

[He] P. Henrici, *Applied and Computational Complex Analysis, Vol.* III, Wiley, New York, 1986.

[Hoi] H.-P. Hoidn, *Osculation methods for the conformal mapping of doubly connected regions*, Z. Angew. Math. Phys., 33 (1982), pp. 640–652.

[LM] P. Luchini and F. Manzo, *Flow around simply and multiply connected bodies: A new iterative scheme for conformal mapping*, AIAA J., 27 (1989), pp. 345–351.

[Lu] L. G. Luenberger, *Linear and Nonlinear Programming*, 2nd ed., Addison–Wesley, Reading, MA, 1984.

[SW] D. B. Szyld and O. B. Widlund, *Variational analysis of some conjugate gradient methods*, East-West J. Numer. Math., 1 (1993), pp. 51–74.

[Weg1] R. Wegmann, *Convergence proofs and error estimates for an iterative method for conformal mapping*, Numer. Math., 44 (1984), pp. 435–461.

[Weg2] R. Wegmann, *On Fornberg's numerical method for conformal mapping*, SIAM J. Numer. Anal., 23 (1986), pp. 1199–1213.

[Weg3] R. Wegmann, *An iterative method for the conformal mapping of doubly connected regions*, J. Comput. Appl. Math., 14 (1986), pp. 79–98.

[Weg4] R. Wegmann, *Discrete Riemann-Hilbert problems, interpolation of simply closed curves, and numerical conformal mapping*, J. Comput. Appl. Math., 23 (1988), pp. 323–352.

[Weg5] R. Wegmann, *Fast conformal mapping of an ellipse to a simply connected region*, J. Comput. Appl. Math., 72 (1996), pp. 101–126.

[Wid] O. Widlund, *On a numerical method for conformal mapping due to Fornberg*, unpublished.